Available online at www.sciencedirect.com

ScienceDirect

Procedia Engineering 10 (2011) 2560–2565

Engineering Procedia

ICM11

Numerical study of the inter-fibre failure under biaxial loads

E. Correa*, F. París, V. Mantič

Group of Elasticity and Strength of Materials, School of Engineering, University of Seville, Camino de los Descubrimientos s/n, 41092 Sevilla, Spain

Abstract

The inter-fibre/matrix failure under transverse tension has already been the object of several micromechanical studies by the authors, for single fibre case or dilute packing. These studies have made it possible to understand the initiation and later progress of failure at the micromechanical scale, which leads to the macro-failure of the material. The generation of damage at this scale is directly associated to the appearance of small debonds or interface cracks at the fibre-matrix interfaces. In the present work the influence, at micro scale, of a secondary transverse load perpendicular to the transverse tension nominally responsible for the failure, is studied for all phases of the mechanism of damage. Both signs of the secondary load, tension and compression, are considered in this analysis. The Boundary Elements Method is employed and Interfacial Fracture Mechanics concepts used for the analysis of the results.

Keywords: Micromechanics; Interfacial Fracture Mechanics; Matrix/inter-fibre failure; Debond; Biaxial loads.

1. Introduction

The studies carried out by the authors about the inter-fibre failure under uniaxial tension, París et al. [1], allowed the first stages of the mechanism of damage at micro level to be identified, showing that it starts with the appearance of small debonds at the fibre-matrix interfaces. These debonds grow unstably along the interfaces until they have reached a certain length, matching with the appearance of a physically relevant contact zone at the tip. From that moment on the growth becomes stable, favouring the kinking towards the matrix. The coalescence between different kinked cracks leads to the final macro-failure.

Many of the existing proposals for the prediction of the inter-fibre at lamina level are based on the hypothesis that the failure taking place at a plane is governed by the components of the stress vector

* Corresponding author. Tel.: 34 954 48 72 99; fax: 34 954 46 16 37.
E-mail address: correa@esi.us.es

 doi:10.1016/j.proeng.2011.04.422

associated to that plane. In the present work this assumption is revised for the tension dominated matrix failure by means of single-fibre Boundary Element models. An analysis of the influence of an out-of-failure plane stress component (tension or compression) on the generation of the damage is carried out. Several aspects of this problem have already been analysed in París et al. [2]. Interfacial Fracture Mechanics, Mantič et al [3], has been used to analyse the results.

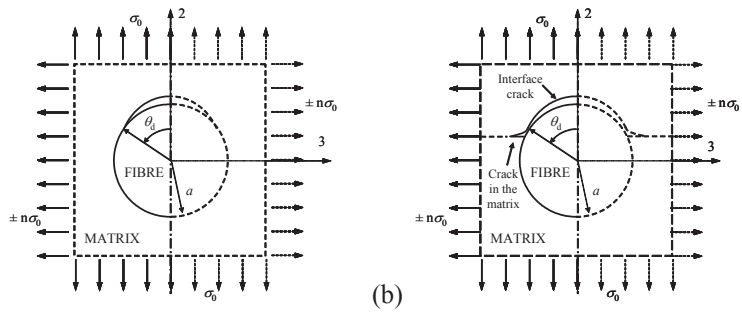

Fig. 1. Single fibre BEM models: (a) with interface crack only, and (b) with interface kinked crack.

2. Modelling

The study has been carried out using a tool based on BEM, París and Cañas [4], that enables to analyse plane elastic problems considering frictionless contact and interface cracks, Graciani et al. [5]. Two BEM models are used in this analysis. The basic one, Fig. 1a, represents the case of an interface crack which, under the plain strain hypothesis, grows symmetrically to axis 2.

To characterize the problem from the Fracture Mechanics point of view the Energy Release Rate, G, will be used. The expression employed, based on the VCCT, Irwin [6], for a circular crack that propagates from a certain debonding angle, θ_d, Fig. 1a, to $\theta_d + \Delta\theta_d$ ($\Delta\theta_d << \theta_d$), is:

$$G(\theta_d, \Delta\Delta_d) = \frac{1}{2\Delta\theta_d}\int_0^{\Delta\theta_d}\left[\sigma_{rr}(\theta_d+\theta)\Delta u_r(\theta_d-\Delta\theta_d+\theta)+\sigma_{r\theta}(\theta_d+\theta)\Delta u_\theta(\theta_d-\Delta\theta_d+\theta)\right]d\theta \qquad (1)$$

θ being the circumferential coordinate referring to axis 2. σ_{rr} and $\sigma_{r\theta}$ represent, respectively, radial and shear stresses at the interface, and Δu_r and Δu_θ are the relative displacements of the crack faces.

Table 1. Elastic properties of the materials.

Material	Poisson coefficient, ν	Young modulus, E
Matrix (epoxy)	$\nu^m = 0.33$	$E^m = 2.79\times10^9\,Pa$
Fibre (glass)	$\nu^f = 0.22$	$E^f = 7.08\times10^{10}\,Pa$

When the presence of an incipient crack in the matrix is considered the previous model is altered to represent a crack that has first grown along the interface and, once kinked into the matrix, is progressing through it, Fig. 1b. The materials chosen for the analysis correspond to a glass fibre-epoxy matrix system, whose elastic properties are included in Table 1. The fibre radius considered has been $a = 7.5\cdot10^{-6}\,m$.

Dimensionless results for G will be presented, obtained, following Toya [7] and Murakami [8], by dividing the values of G by $G_0 = \left((1+\kappa^m)/8\mu^m\right)\sigma_0^2 a\pi$, where $\kappa^m = 3-4\nu^m$, μ^m is the shear modulus of the matrix and σ_0 is the external applied tension.

3. Origin of failure

The initiation of the failure at the interface has been considered to be controlled by the σ_{rr} distribution, Goodier [9], at the undamaged interface. Then it is fundamental to analyze the influence that the different levels of σ_{33} have on σ_{rr} of the undamaged interface. Three different values of *n* coefficient have been considered: *0*, *0.5* and *1*. The notation employed to distinguish between the different biaxial cases follows the scheme: T-*n*C and T-*n*T (T=tension, C=compression).

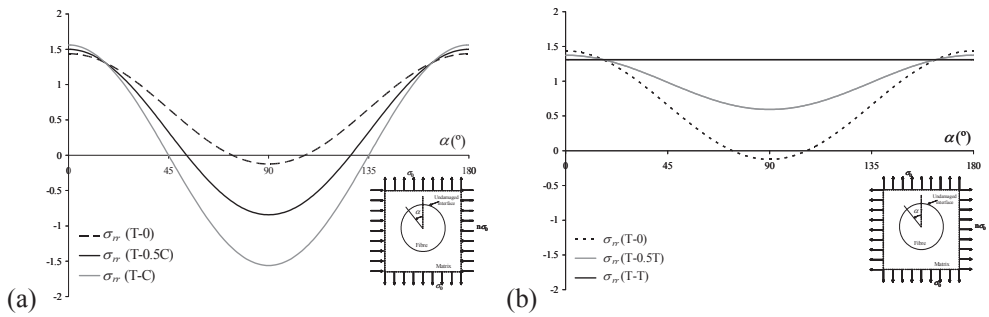

Fig. 2. (a) σ_{rr} distribution (T-*n*C case); (b) σ_{rr} distribution (T-*n*T case).

Curves presented in Fig. 2a (T-*n*C case) show that the presence of σ_{33} does not qualitatively alter the distribution of σ_{rr}. Quantitatively, with reference to the T-0 case, compressive σ_{rr} significantly increases as σ_{33} does, whereas maximum tensile σ_{rr} increases only slightly. Referring to the T-*n*T case, Fig. 2b, the σ_{rr} level at the interface is maintained with reference to the T-0 case though the tendency generated is to level the σ_{rr} state between all interfacial points, as is shown in T-T case. Based on this, an initial debond at the interface of 10º length centred in axis 2 (position at which σ_{rr} is maximum) will be assumed for the study of the interface crack, both for the T-*n*C and the T-*n*T case.

4. Interfacial crack growth

The evolution of the first debond at the interface is studied by means of the BEM model shown in Fig. 1a and its growth evaluated in terms of the Energy Release Rate, G, Eq. (1).

4.1. Tension-compression biaxial case

The results obtained show that the presence of $\sigma_{33} < 0$ does not qualitatively alter the evolution of G versus θ_d, though it is found that its level increases as $\sigma_{33} < 0$ does, which means that the load level required for crack propagation is lower.

The prediction of growth of the interface crack is made by comparing G with its corresponding critical value, G_c, Hutchinson and Suo [10]. G - G_c comparisons for the cases T-0 and T-C (representative of all T-*n*C cases) are plotted in Fig. 3a. $\lambda = 0.2$ has been chosen and G_{1c} has been taken as the value that makes G and G_c coincide for the first debonding angle, $\theta_d = 10^o$ in this case. This criterion can be implemented once a scaled representation of the G curves, that makes all curves to

coincide at $\theta_d = 10^o$, has been considered. The results predict an unstable growth of the interface crack that reaches lower θ_d as the presence of $\sigma_{33} < 0$ increases, though the value of σ_0 needed for the initiation of the crack growth is lower as $\sigma_{33} < 0$ increases. This means that the presence of a compression superimposed on the tension nominally responsible for the failure accelerates the failure, in accordance with the results obtained from experimental tests [2].

4.2. Tension-tension biaxial case

The results obtained for this case show that the presence of $\sigma_{33} > 0$ does not significantly alters the G level obtained in the T-0 case, though a translation of the position of the maxima has been detected. It can also be deduced that the propagation of the initial debond requires a slightly higher level of the external load as n increases. G and G_c curves associated to T-nT cases corresponding to $n=0,0.5$ and 1 are represented together in Fig. 3b. The results obtained predict an unstable growth of the interface crack that extends towards larger θ_d as the presence of $\sigma_{33} > 0$ increases, though the amount of load required for the initiation of growth is also slightly greater as this presence increases. For the T-T limit case this tendency could lead to a particularly large extension of the crack at the interface that, in conjunction with the special morphology of the crack detected in this case (consisting in the opening of the previously developed contact zone near the tip), would impede the kinking of the crack towards the matrix.

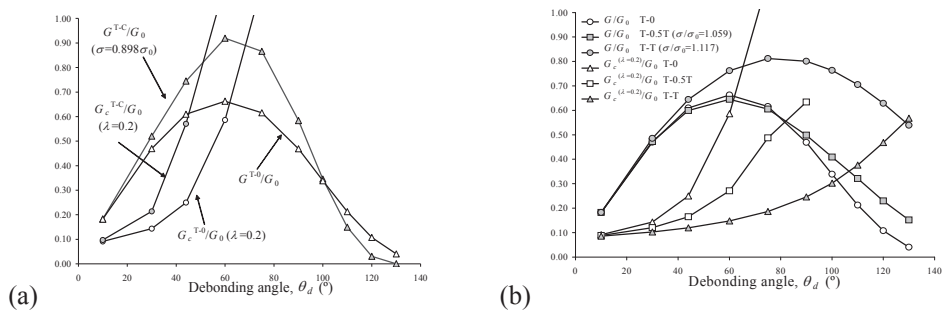

Fig. 3. (a) G-G_c comparison (T-nC case). (b) G-G_c comparison (T-nT case).

5. Kinking

The stable position reached by the crack at the interface after a period of unstable growth warns about the possible occurrence of a different stage in the mechanism of damage: the kinking towards the matrix.

The first step of the kinking analysis consists in the study of the circumferential stress around the interface crack tip in order to identify the preferential direction of kinking, associated to the maximum circumferential stress, $\sigma_{\theta\theta}^{max}$, for each position of the interface crack, according to the Maximum Circumferential Stress Criterion [11]. In addition, an energetic evaluation of the propagation of the crack in the matrix, once kinked, has been carried out.

5.1. Tension-compression biaxial case

Using the model of Fig. 1a the distribution of $\sigma_{\theta\theta}$ has been evaluated for interface crack tips corresponding to θ_d in the range [30^o-90^o] and 3 different distances, r, to the crack tip [$0.001a$, $0.005a$,

0.01a]. The results obtained for the T-C case show that $\sigma_{\theta\theta}^{max}$ takes place for $\theta_d = 60^o$. With reference to the orientations associated to $\sigma_{\theta\theta}^{max}(\theta_d)$, $\theta(\sigma_{\theta\theta}^{max})$, Fig. 4a, the results show a weak dependence on *r*. Besides, $\theta(\sigma_{\theta\theta}^{max})$ coincides with the expected macromechanical orientation of failure, 90^o, for $\theta_d = 70^o$.

Once the preferential kinking direction of the interface crack has been calculated it is necessary to study, [1], the kinking occurrence from an energetic point of view. To this end the model shown in Fig. 1b has been used and the presence of a small kinked crack, oriented parallel to axis 3, has been considered for different θ_d. G values associated to the different kinked cracks have been calculated and represented in Fig. 4b versus θ_d. G evolution of the interface crack for the T-C case has been also included here.

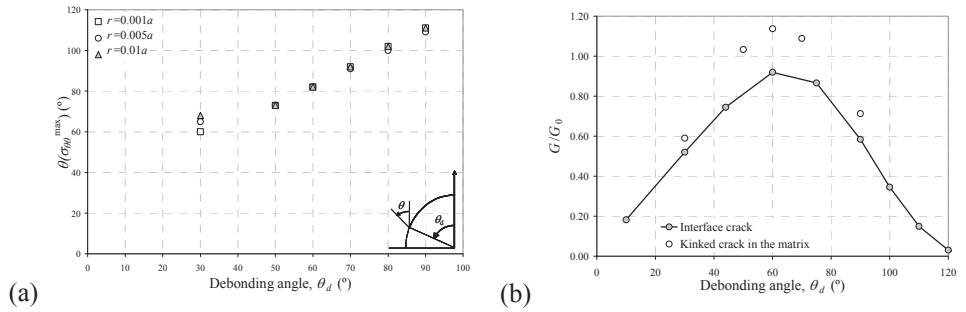

Fig. 4. T-C case (a) $\theta(\sigma_{\theta\theta}^{max})$ predictions versus θ_d .(b) G comparison between the interface crack and kinked cracks.

The results obtained show that for the θ_d range employed, the G value of the kinked crack is greater than the corresponding G of the interface crack. It can also be detected that the maximum differences are found for θ_d whithin the range of ending of unstable growth at the interface. For the angle of interest, $\theta_d = 70^o$, it can also be demonstrated that, if kinking takes place the later growth of the crack in the matrix is unstable and in Mode I. Finally, for the bi-material system under study it can be considered that the critical value of G_{II} associated to the interface is greater than the critical value of G_I associated to the matrix. Thus, based on the relative values of G_c for the interface and the matrix and the different character of growth for both possibilities: unstable and in Mode I for the matrix, and stable and in Mode II for the interface, favourable conditions are found for the kinking of the interface crack towards the matrix once it has reached a stable position at the interface.

5.2. Tension-tension biaxial case

For the sake of simplicity, the study will be limited to the T-0.5T case and identical procedure will be employed as in the T-C case.

Referring to the search of the preferential direction of kinking, Fig. 5a shows the values obtained for $\theta(\sigma_{\theta\theta}^{max})$ versus θ_d for the three distances *r* considered. The results show that, as happens for the T-0 case, $\theta(\sigma_{\theta\theta}^{max})$ varies in an approximated range of $70^o \le \theta \le 110^o$, the global maximum being located at $\theta_d = 60^o - 70^o$ and associated to a direction that coincides with the expected macro orientation of failure. Based on these results, if kinking at the range of ending of instable growth at the interface occurred, it would take place in the direction perpendicular to the dominant external tension.

Finally, the comparison between G of the kinked crack and G of the interface crack is shown in Fig. 5b. Higher values are found for the kinked crack than for the interface one in the range of interest. Thus, based on the relative values of G_c for the interface and the matrix and the growth character of both possibilities, the kinking towards the matrix is expected once a stable position at the interface is reached.

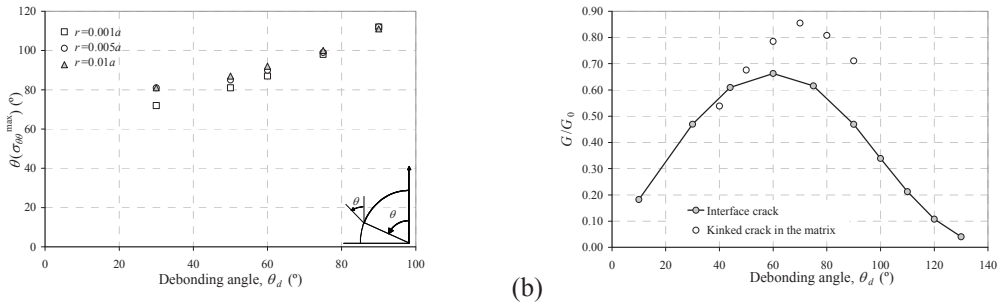

Fig. 5. T-0.5T case (a) $\theta(\sigma_{\theta\theta}^{max})$ predictions versus θ_d, (b) G comparison between the interface crack and kinked cracks.

6. Conclusions

The first stages of the development of the tension dominated inter-fibre failure under biaxial loads have been studied by means of a single fibre BEM model. A secondary external load has been considered to act simultaneously with the tension nominally responsible for the failure, and both cases (tension and compression) have been analysed. The results obtained show that the presence of a secondary load could alter several aspects of the stages already detected for the tension uniaxial case leading then to the conclusion that the presence of an out plane stress component could affect the development of the failure.

Acknowledgements

The work was supported by the Spanish Ministry of Education and Science (TRA2005-06764, TRA2006 08077 and MAT2009-14022) and Junta de Andalucía (TEP-02045 and TEP-04051). The authors thank Dr. E. Graciani (University of Seville) whose BEM code has been used.

References

[1] París F, Correa E, Mantič V. Kinking of transverse interface cracks between fibre and matrix. *J App Mech* 2007;**74**:703–716.

[2] París F, Correa E, Cañas J. Micromechanical view of failure of the matrix in fibrous composite materials. *Compos Sci Technol* 2003;**63**:1041–1052.

[3] Mantič V, Blázquez A, Correa E, París F. Analysis of interface cracks with contact in com-posites by 2D BEM. In: Guagliano M, Aliabadi MH, editors. *Fracture and Damage of Composites*, Southampton: WIT Press; 2006, p. 189–248.

[4] París F, Cañas J. *Boundary Element Method. Fundamentals and Applications*. Oxford: OUP; 1997.

[5] Graciani E, Mantič V, París F, Blázquez A. Weak formulation of axi-symmetric frictionless contact problems with boundary elements. Application to interface cracks. *Comput Struct* 2005;**83**:836-855.

[6] Irwin GR, Analysis of stresses and strain near the end of a crack transversing a plate. *J App Mech* 1957;**24**:361–4.

[7] Toya M. A crack along the interface of a circular inclusion embedded in an infinite solid. *J Mech Phys Solids* 1974;**22**:325–348.

[8] Murakami Y. *Stress Intensity Factor Handbook*. Oxford: Pergamon Press; 1988.

[9] Goodier JN. Concentration of stress around spherical and cylindrical inclusions and flaws. *App Mech* 1933;**55**:39–44.

[10] Hutchinson JW, Suo Z. Mixed mode cracking in layered materials. *Adv App Mech* 1992;**29**:63–191.

[11] Erdogan F, Sih GC. On the crack extension in plates under plane loading and transverse shear. *J Basic Eng* 1963;**85**:519–527.